JOURNAL OF THERMOPHYSICS AND HEAT TRANSFER
Vol. 8, No. 3, July–Sept. 1994

# High-Temperature, Normal Spectral Emittance of Silicon Carbide Based Materials

Michael A. Postlethwait,* Kamal K. Sikka,* Michael F. Modest,† and John R. Hellmann‡
*Pennsylvania State University, University Park, Pennsylvania 16802*

**An emissometer was designed and constructed to measure the normal, spectral emittance of opaque solids over the spectral range from 1 to 8 $\mu$m for temperatures ranging from 500 to 1500°C using an integral blackbody technique. The emissometer is gas-tight so that the gas environments surrounding the sample can be controlled and emittance data can be collected as a function of exposure time to a specific environment at a particular temperature. An FT-IR spectrometer collects the blackbody and sample infrared signals, which are ratioed to calculate the material's emittance. A computer code was developed to check the validity of the assumptions associated with the measurement technique. The emittance of silicon carbide in the form of $\alpha$-SiC (Hexoloy SA) and $TiB_2$-toughened SiC (Hexoloy ST) was collected over the spectral and temperature ranges given above. The emittance for Hexoloy SA was measured in the as-received condition and after sample exposure at 1300°C to carburizing, oxidizing, and low-pressure nitrogen environments. Emittance data for Hexoloy ST were collected for samples in the as-received condition and for samples exposed to oxidizing environments. The surface morphology and composition of the samples were characterized using SEM, EDX, and X-ray diffraction techniques.**

## Nomenclature

| | | |
|---|---|---|
| $C_1$, $C_2$, $C_3$ | = | correction factors for systematic errors, – |
| $d$ | = | layer thickness, $\mu$m |
| $E$ | = | emissive power, W/m$^2$ |
| $F_{i-j}$ | = | view factor, from $A_i$ to $A_j$ |
| $H$ | = | irradiation, W/m$^2$ |
| $I$ | = | radiation intensity, W/m$^2$sr |
| $n$ | = | index of refraction, – |
| $S$ | = | signal strength, mV |
| $\hat{s}$ | = | unit direction vector, – |
| $T$ | = | temperature, K |
| $\varepsilon$ | = | emittance |
| $\theta$ | = | polar angle, rad |
| $\lambda$ | = | wavelength, $\mu$m |
| $\phi$ | = | azimuthal angle, rad |

*Subscripts*

| | | |
|---|---|---|
| $b$ | = | blackbody |
| bg | = | background |
| $i$ | = | incident |
| $m$ | = | measured |
| $s$ | = | sample |
| ss | = | stainless steel drop tube |
| $\lambda$ | = | spectral value, per unit wavelength |

## Introduction

NEW ceramic composites are continually being developed to meet the industrial need for high-strength materials capable of withstanding extreme temperatures. One group of ceramic materials, which has recently received increased attention with advances in processing techniques, is the silicon carbide group. The low coefficient of thermal expansion and high thermal conductivity of silicon carbide make the material highly resistant to thermal shock and, therefore, ideally suited for many high-temperature applications, including indirect gas-fired heating systems, heat engine applications, waste heat recovery systems, etc. The silicon carbide components utilized in these applications are exposed to a wide variety of gaseous environments, which may be highly corrosive, oxidizing or reducing in nature.

With the advent of these new materials and their corresponding applications, it has become imperative to characterize the physical properties of these materials and understand how these properties vary for different applications.[1,2] The need for thermal radiation property data is twofold: their availability not only facilitates a great number of thermal design computations, but also makes pyrometric or thermographic measurement techniques feasible.[3] One such radiative property, which is of key importance in radiative heat transfer, is emittance.

The emittance of a material can be a function of the material temperature, direction of emission, and wavelength. The spectral, directional emittance of an opaque surface is defined as

$$\varepsilon'_\lambda(T, \lambda, \hat{s}) \equiv \frac{I_\lambda(T, \lambda, \hat{s})}{I_{b\lambda}(T, \lambda)} \tag{1}$$

which is a ratio of the spectral, directional emitted intensity, leaving a surface at a particular temperature $T$, and wavelength $\lambda$, into a direction $\hat{s}$, and the spectral, directional emitted intensity leaving a blackbody at the same temperature and wavelength. If emittance does not vary with direction, the surface is considered to be a diffuse emitter. Dielectrics with isotropic surface characteristics (i.e., most ceramics) can be classified as diffuse emitters since the emissivity remains fairly constant over all directions except for large grazing angles. In these directions only small amounts of energy are emitted as compared to the total emitted energy of the surface. For a diffuse emitter the above expression is no longer directionally dependent.

Because the emittance of a material is primarily a surface phenomenon, the surface morphology and composition of the material can have significant effects on corresponding emittance values. Methods of preparation, surface finish, aging,

Received June 28, 1993; presented as Paper 93-2759 at the AIAA 28th Thermophysics Conference, Orlando, FL, July 6–9, 1993; revision received Nov. 5, 1993; accepted for publication Nov. 10, 1993.


*Research Assistant, Department of Mechanical Engineering, Room 110 Hallowell Bldg.
†Professor, Department of Mechanical Engineering, Room 211 Hallowell Bldg. Member AIAA.
‡Assistant Professor, Department of Materials Science and Engineering, Room 511 Deike Bldg.

interactions with the environment, etc., can significantly alter the surface characteristics of the material, and thus alter its emittance. The difficulty in controlling and specifying the surface characteristics of a material causes appreciable differences between measured emittance values and the values predicted by many refined theories. In order to unambiguously relate the measured emittance data to the conditions of the material and to understand environmental influences, it is necessary to measure the emittance of the actual material in the environment of its application.

Touloukian and DeWitt[4-6] have prepared an exhaustive compilation of emittance data for a wide range of materials. Chaney et al.[7] have compiled another comprehensive listing of emittance literature through 1980. Richmond[8] and Katzoff[9] collected all relevant literature on experimental methods for emittance measurements when the interest in this area was at its peak in the 1960s due to the advent of the space age. Interest waned in the subsequent decade but has picked up again recently due to the development of new high-temperature materials. Sacadura[3] has surveyed the metrological developments, which have taken place in this area through 1986.

Generally, emittance can be measured directly or indirectly. Direct methods include calorimetric and emission measurement techniques, whereas indirect methods are based on reflectance measurements. Reflectance measurement methods have generally been limited to lower temperatures, whereas calorimetric methods are limited to the measurement of total emittance. Direct emission measurement techniques require the comparison of sample emission with blackbody emission under exactly the same conditions. The comparison blackbody may either be a separate blackbody at the same temperature or an integral blackbody cavity. The latter is usually preferred at high temperatures, where temperature measurement and control are difficult, and at very short wavelengths, where extremely close temperature control is required for accurate measurement. Consequently, the integral blackbody measurement technique was chosen as the appropriate method of measurement of normal, spectral emittance for elevated temperatures.

Three choices were identified for alternately viewing the sample and the integral blackbody emissions. These included the linear actuation of the sample in the blackbody compartment,[10] the rotation of the sample and blackbody under a cold viewing port,[11] or the dropping of a cold sight tube.[12] Linear actuation makes it extremely difficult to keep the sample at the same temperature for different positions in the blackbody compartment. Rotation of the sample and the blackbody requires an involved cooling system to assure that the viewing port remains cold. In addition, rotation at high temperatures can cause thermal shock problems for the ceramic samples. Thus, the basic emissometer design of Vader et al.[12] was deemed as the most suitable for normal spectral emittance measurements over the spectral range from 1 to 8 $\mu$m and the temperature range of 500 to 1500°C.

Several main differences exist between Vader's design and the apparatus outlined in this article. With this design, the sample chamber can be purged to control the high-temperature environments surrounding the sample, and the sample holder can be removed to facilitate the changing of samples. This design also uses an FT-IR spectrometer for signal detection and in the design by Vader et al.,[12] a monochromatic radiometer is used. With the FT-IR spectrometer emittance data can be collected over the entire spectral range of interest with a single measurement, however, with a monochromatic radiometer, data must be collected at each individual wavelength, making the collection process much more time consuming.

## Experimental Setup and Procedure

In the integral blackbody technique, the emittance is determined by placing the sample in a heated isothermal cylindrical cavity with sufficient aspect ratio such that the cavity functions as a blackbody.[13] A blackbody signal is then collected. Immediately following the blackbody measurement, a "cold" tube is dropped into the cavity, thus blocking all side wall radiation, so that only emission from the sample is viewed. At this instant, the sample signal is collected. After subtracting unwanted background radiation from each signal, the resulting sample signal is then divided by the corrected blackbody signal to yield the normal spectral emittance of the sample at the temperature of the cavity. Based on the integral blackbody technique, the emissometer assembly (Fig. 1), which consists of an airtight furnace assembly and dropping mechanism, a temperature controller, the optical path, and an FT-IR was fabricated. The furnace assembly consists of a vertical tube furnace with hot zone capable of reaching temperatures up to 1550°C. The cylindrical cavity passing through the bore of the furnace consists of a SiC tube with brass seals at both ends for sealing purposes. This large silicon carbide tube functions as the sample chamber. Placed concentrically within the SiC tube is another SiC tube, which functions as the blackbody cavity with an aspect ratio of 4.5. A removable SiC rod seated in machined alumina brick within the larger tube serves as a pedestal for sample placement. A bore through the upper brass seal allows for the passage of the cold drop tube into the heated blackbody cavity. A sheathed S-type thermocouple was placed in contact with the underside of the sample to monitor the sample and blackbody temperature. Figure 2 provides an assembled view of the sample chamber.

The drop tube and the drop tube mechanism are enclosed in an airtight aluminum housing, which is positioned precisely over the upper brass seal. The drop tube mechanism was designed for the quick and repeatable placement of the cold drop tube into the blackbody cavity by allowing the tube to free-fall to the correct position where pneumatic dampers are used to reduce unwanted shock and vibration. Following the collection of the sample signal, the tube is then retracted from the cavity. The quick placement of the cold drop tube is critical since heating of the cold tube as well as cooling of the sample must be minimized to assure accurate emittance measurements.

An optical port at the top of the aluminum housing allows the emission signals of sample and blackbody to be passed

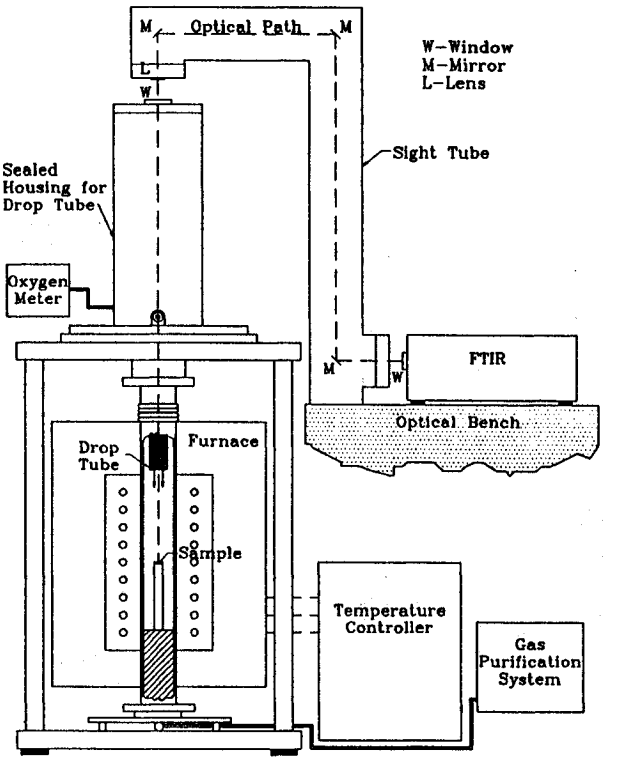


Fig. 1 Emissometer assembly.

**Table 1 Various heat treatments evaluated for emittance measurements of Hexoloy SA and ST**

| Material/treatment | Treatment, volume % | Length of treatment, h | Treatment temperature, °C | Treatment pressure, Torr |
|---|---|---|---|---|
| Hexoloy SA: as-received | No treatment | — | — | — |
| Hexoloy SA: carburizing | 40 $H_2$, 38 $N_2$, 22 CO | 24 | 1300 | 760 |
| Hexoloy SA: low-pressure $N_2$ | 98.2 $N_2$, 0.6 CO, 0.2 $H_2$ | 24 | 1300 | 1 |
| Hexoloy SA: oxidizing | 100 $O_2$ | Variable | 1300 | 760 |
| Hexoloy ST: as-received | No treatment | — | — | — |
| Hexoloy ST: oxidizing | 100 $O_2$ | Variable | 1300 | 760 |

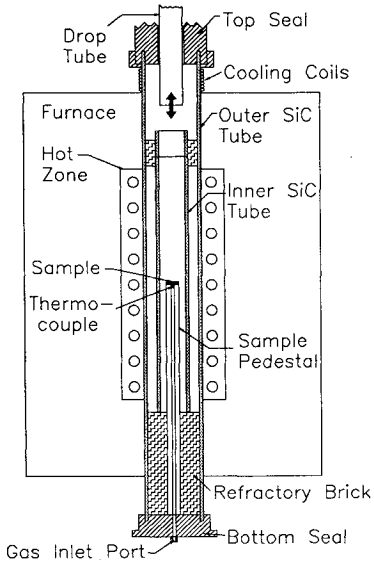


**Fig. 2 Assembled view of the sample chamber.**

through a lens, an aperture, and a series of flat mirrors, which directs the signals into the opening of the FT-IR spectrometer. The spectrometer then collects the signals over the spectral range from 1 to 8 $\mu$m, using a Fast Fourier Transform to convert the collected interferogram into spectral intensities. With the FT-IR spectrometer, data are collected over the spectral range of interest in a time frame of approximately 2 s for each blackbody and sample reading. The spectral data are averaged over eight scans of the spectrometer's moving mirror using a 16-$cm^{-1}$ resolution.

The emittance of Hexoloy SA samples was collected for samples in the as-received condition (sintered $\alpha$-SiC), and for samples exposed to low-pressure nitrogen, carburizing and oxidizing environments for temperatures ranging from 500 to 1500°C. For the low-pressure $N_2$ and carburizing treatments, the SA samples were pretreated in the environments and then the emittance measurements were made in an inert, helium atmosphere. The emittance data for Hexoloy ST were collected for the materials in the as-received condition (sintered $\alpha$-SiC with approximately 15% volume of $TiB_2$) and during sample exposures to oxidizing environments. The oxidation studies for both Hexoloy SA and ST were carried out within the emissometer. In order to study the effects of oxidation on emittance, the samples were heated to 1300°C in a helium environment and then the emissometer was purged with dry oxygen and emittance was measured as a function of exposure time to oxygen. Table 1 provides a description of the parameters for each heat treating environment.

To limit surface modifications to the sample from reactive species within the sample chamber, the system was continuously purged in an inert gas atmosphere with oxygen partial pressures less than $10^{-10}$ atm. Low levels of oxygen were achieved through a gettering/purification system and measured with an oxygen analyzer. The purification system also removed other impurities typically found in nitrogen and helium purge gases, including hydrocarbons, CO, $CO_2$ and water vapor. For oxidation studies, the sample was treated within the furnace using a pure dry oxygen purge. The oxygen levels within the sample chamber were monitored periodically during data collection to determine whether the sample was undergoing active or passive oxidation. Active oxidation is characterized by the loss in material weight stemming from emission of SiO gas. During passive oxidation, oxygen reacts with silicon to form a silica layer on the silicon carbide substrate. Figure 3[14] displays the oxygen partial pressures associated with the transition from active to passive oxidation for silicon carbide.

Before and after emittance data were collected for a given sample, its surface morphology and composition were evaluated using scanning electron microscopy and x-ray diffraction techniques.

## Data Reduction and Evaluation

As defined previously, directional spectral emittance is the ratio of the sample and blackbody emission signals at the same particular wavelength and in the same particular direction. However, it is not possible to measure this quantity exactly. Rather, the emission signals are collected over a small solid angle, over which the spectral intensity $I_\lambda$ is assumed to be constant (for this setup a half-angle of $\Delta\phi \leq 4.5$ mrad defines the field of view for the detector). Therefore, the measured emittance for a particular solid angle and wavelength can be expressed as

$$\varepsilon(\lambda, \theta, \phi, T) \cong \frac{\int_{\theta_1}^{\theta_2}\int_{\phi_1}^{\phi_2} I_\lambda(\lambda, \theta, \phi, T)\sin\theta \, d\phi \, d\theta}{\int_{\theta_1}^{\theta_2}\int_{\phi_1}^{\phi_2} I_{b\lambda}(\lambda, T)\sin\theta \, d\phi \, d\theta} \quad (2)$$

Since $I_\lambda(\lambda, \theta, \phi, T)$ may be assumed to be constant over very small solid angles it can be taken outside the integral, and Eq. (2) reduces to the definition of emittance, Eq. (1). Thus, the data reduction procedure involves taking the ratio of the collected sample and blackbody emission signal to obtain the measured normal, spectral emittance $\varepsilon_m$. This ratio can be written as

$$\varepsilon_m(\lambda, T) = \frac{S_s - S_{bg}}{S_b - S_{bg}} \quad (3)$$

where $S_s$ is the signal due to the spectral energy received at the detector when the drop tube is at its bottom position, $S_b$ is the corresponding signal when the drop tube is outside the blackbody cavity and $S_{bg}$ is the background spectral signal. It was found that the maximum intensity of background signal is of the same order of magnitude as the noise associated with the FT-IR.

The emittance as determined from Eq. (3) is subject to the following assumptions:

1) The blackbody is perfectly black (i.e., the emissive power of the blackbody cavity is equivalent to that of a blackbody at the sample temperature). This assumes that the blackbody cavity is isothermal (at the temperature of the sample) and that the isothermal zone has a sufficient aspect ratio such that the emissivity of the cavity is unity.

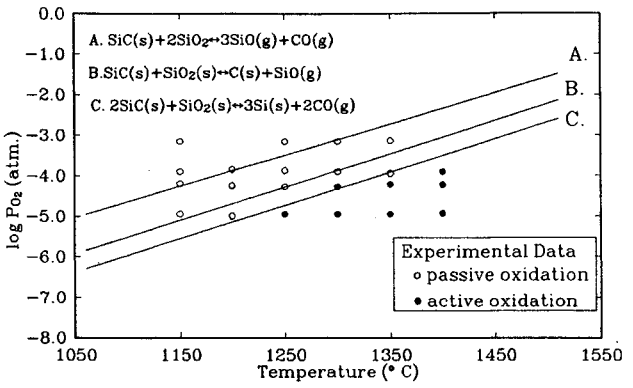


**Fig. 3 Oxygen partial pressures associated with the transition from active to passive oxidation for silicon carbide. Lines A, B, and C represent the theoretical transition lines and the symbols represent experimental data for active and passive oxidation.[14]**

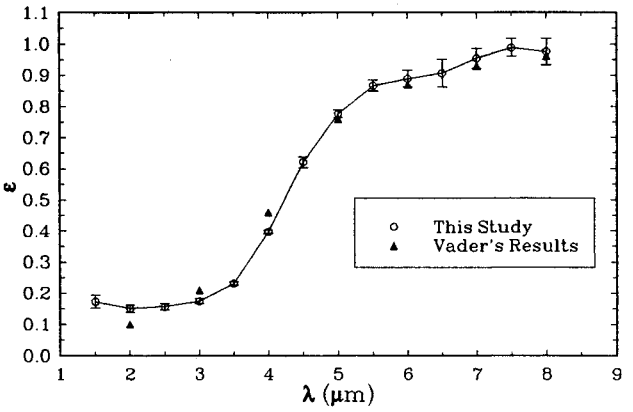


**Fig. 4 Comparison of Coors AD995 alumina results with Vader's results at 1020°C. (Error bars represent a 95% confidence interval for a single measurement.)**

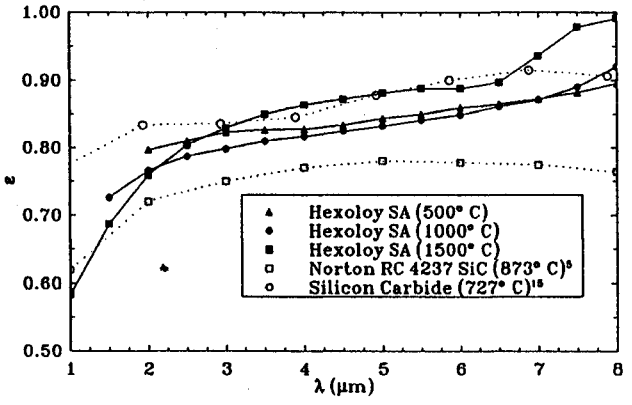


**Fig. 5 Normal, spectral emittance of Hexoloy SA (as-received) and other SiC-based materials (previously published results) for various temperatures.**

2) When the drop tube is inserted into the cavity, it neither emits nor reflects radiation back toward the sample, thus augmenting the true sample signal.

3) The sample remains isothermal during the collection of the blackbody and sample signals.

In order to assess the validity of these assumptions during the collection of emittance data, the following procedure was developed to re-estimate the sample emittance based upon the actual conditions of the measuring technique. The sample and blackbody emission signals can be written as

$$S_s - S_{bg} = F_d[\varepsilon_\lambda E_{b\lambda}(T_s) + (1 - \varepsilon_\lambda)H_{ss,\lambda}] \quad (4)$$

$$S_b - S_{bg} = F_d[\varepsilon_\lambda E_{b\lambda}(T_b) + (1 - \varepsilon_\lambda)H_{b\lambda}] \quad (5)$$

where $E_{b\lambda}$ is the spectral blackbody emissive power, $H_{ss,\lambda}$ is the irradiation onto the sample from the drop tube, and $H_{b\lambda}$ is the irradiation onto the sample from the SiC blackbody walls. $T_s$ is the sample temperature when the drop tube is down, and $T_b$ is the sample temperature when the tube is up. The proportionality constant $F_d$ is related to the view factor from the sample or the blackbody to the detector and includes the combined effects of attenuation and augmentation from the gases along the optical path, detector responsivity, absorptance of the mirrors, and transmittance of the lens and windows. $\varepsilon_\lambda$ is the true spectral emittance of the sample.

From Eq. (3), the measured spectral emittance can then be expressed as

$$\varepsilon_{m,\lambda} = \frac{F_d[\varepsilon_\lambda E_{b\lambda}(T_s) + (1 - \varepsilon_\lambda)H_{ss,\lambda}]}{F_d[\varepsilon_\lambda E_{b\lambda}(T_b) + (1 - \varepsilon_\lambda)H_{b\lambda}]} \quad (6)$$

The corrected emittance is then obtained from Eq. (6) as

$$\varepsilon = \frac{\varepsilon_m C_1 - C_2}{C_3 - C_2 - \varepsilon_m(1 - C_1)} \quad (7)$$

where

$$C_1 = \frac{H_{b\lambda}}{E_{b\lambda}(T_b)}, \qquad C_2 = \frac{H_{ss,\lambda}}{E_{b\lambda}(T_b)}, \qquad C_3 = \frac{E_{b\lambda}(T_s)}{E_{b\lambda}(T_b)} \quad (8)$$

$C_1$ represents the spectral correction factor for the blackbody not being perfectly black. For the ideal case, the irradiation onto the sample from the blackbody walls $H_{b\lambda}$, equals the spectral emissive power of a blackbody at the sample temperature and, thus, $C_1$ would equal unity. The correction factor $C_2$ accounts for the reflected and emitted radiation of the drop tube, which falls onto the sample. For the ideal case, the irradiation from the drop tube onto the sample $H_{ss}$ would equal zero and, thus, $C_2$ would equal zero. The last correction factor $C_3$, represents the measurement error associated with the drop in sample temperature due to placement of the cold drop tube into the sample chamber. Ideally, the sample temperature should equal the blackbody temperature during the collection of the sample signal and, therefore, $C_3$ should be unity.

A program was developed to estimate the values of $C_1$, $C_2$, and $C_3$, which in turn were used to assess the validity of the assumptions associated with the experimental setup. In the program, the blackbody cavity is treated as a nonisothermal enclosure with varying wall emissivities. The enclosure is divided into $N$ isothermal elements based upon measured cavity temperature profiles. The irradiation onto the sample from the drop tube and the cavity walls is calculated using internodal view factors and nodal radiosities determined from the measured temperatures and the emissivities of the drop tube and cavity. The drop in sample temperature is estimated using a one-dimensional transient heat transfer model. These results are then used in an iterative procedure to calculate $C_1$, $C_2$, and $C_3$. The measured emittance data and the three correction factors for Hexoloy SA were evaluated for temperatures of 500, 1000, and 1500°C, and the results indicated a maximum of 0.2% deviation between corrected and measured emittance values. These results indicate that the systematic errors associated with these assumptions are negligible relative to the estimated uncertainty ($\pm 0.05$) of the instrument.

The emissometer was tested with a well characterized material to ascertain the accuracy and precision of the instrument. The reference material chosen was Coors AD995 alumina. Data collected showed excellent agreement with the previously published data of Vader[12] (Fig. 4). Data were collected several times for the same sample and a high level of repeatability was achieved. The error bars displayed on the graph represent a 95% confidence interval that data from a single measurement of the same sample will fall within the

given range. Scatter in the data was more significant at the limits of the spectral range over which data were collected. This scatter was the result of a lower signal-to-noise ratio in these spectral regions. The large scatter observed at 6.5 $\mu$m was attributed to the strong water vapor absorption bands, which contribute to a low signal-to-noise ratio at this spectral location.

It was not possible to quantify the experimental uncertainty associated with the complex signal processing procedure intrinsic to the workings of the FT-IR spectrometer. The propagation of errors associated with the Fast Fourier transformation of detected signals into spectrally resolved data and the effects of the internal optical path of the FT-IR (including detector nonlinearities) were not quantifiable. Based upon the high repeatability level of the measurement technique, the excellent agreement with published data and the previously discussed analysis of assumptions, an uncertainty level of $\pm 0.05$ emittance units was estimated for this measurement technique.

Emittance data presented in the following section lie within the uncertainty level of the instrument. For lower temperatures, there is a large scatter in the data at shorter wavelengths resulting from the low signal-to-noise over this spectral region. If the scatter exceeded the uncertainty level of $\pm 0.05$ emittance units, the values were not presented. At higher temperatures, the emittance results in the following section approached or exceeded unity at longer wavelengths. There is some question as to whether this trend is a true temperature effect or is due in part to experimental errors associated with detector linearity, however, the presented data are still physically meaningful based on the uncertainty level of the emissometer. Also, published results for single crystal silicon carbide at room temperature show emittance values approaching unity at 9 $\mu$m.[15]

## Discussion of Results

The emittance data of the as-received Hexoloy SA samples displayed a weak dependence on sample temperature. At the shorter (i.e., between 1–2 $\mu$m) and longer wavelengths (between 7–8 $\mu$m) the temperature effects were slightly more pronounced. This trend can be observed in Fig. 5 where the normal, spectral emittance of untreated Hexoloy SA is plotted as a function of wavelength and temperature. The emittance of Hexoloy SA matches well with the silicon carbide data reported in the emittance data base compiled by Touloukian and DeWitt[5] and Incropera and DeWitt.[16] For lower temperatures, emittance data were not plotted at shorter wavelengths due to the low signal-to-noise ratio, which produced large scatter in the data.

For samples exposed to the low-pressure nitrogen and carburizing heat treatments, trends were quite similar to the emittance data collected for the as-received samples for the various temperatures considered. Figure 6 compares emittance data at 1000°C for the treated and untreated samples. The micrographs of the SA samples exposed to the low-pressure nitrogen treatment were very similar to the micrographs of the as-received samples. Slight grain etching and moderate surface pitting was observed on the samples as a result of active oxidation. The micrographs of the samples exposed to carburizing treatments displayed more significant surface modifications as a result of carbon deposition on the sample surface (Fig. 7). However, these changes in surface characteristics did not result in substantial variations in the spectral emittance of the material.

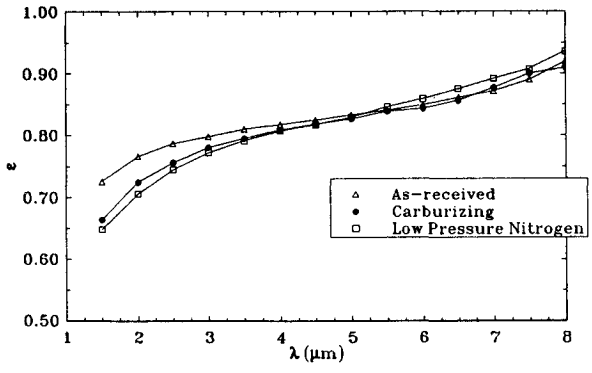


**Fig. 6 Normal, spectral emittance of Hexoloy SA at 1000°C before and after carburizing and low-pressure nitrogen heat treatments.**

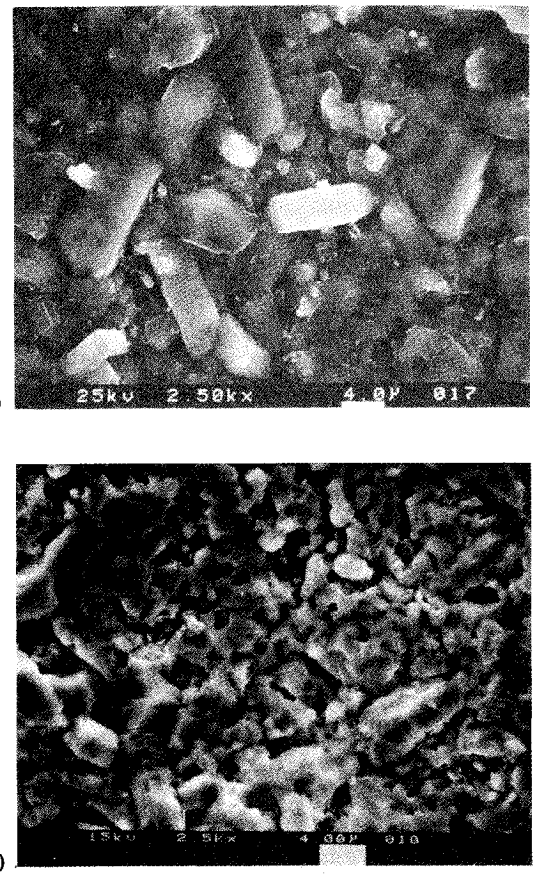


**Fig. 7 SEM microstructure of Hexoloy SA a) in the as-received condition and b) following the carburizing treatment.**

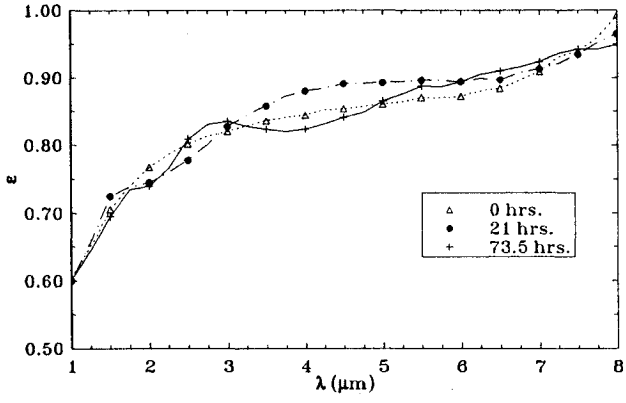


**Fig. 8 Normal, spectral emittance of Hexoloy SA exposed to oxidizing environments for 21 and 73.5 h.**

The emittance data for the SA samples subjected to timed exposures to an oxygen-rich environment at 1300°C did not vary substantially from the as-received emittance data. However, there were noticeable periodic fluctuations in the emittance data at the shorter wavelengths (Fig. 8). These fluctuations in emittance are attributed to interference effects resulting from the formation of a semitransparent vitreous silica layer on the sample surface. Applying electromagnetic wave theory for thin films, the thickness of a uniform thin

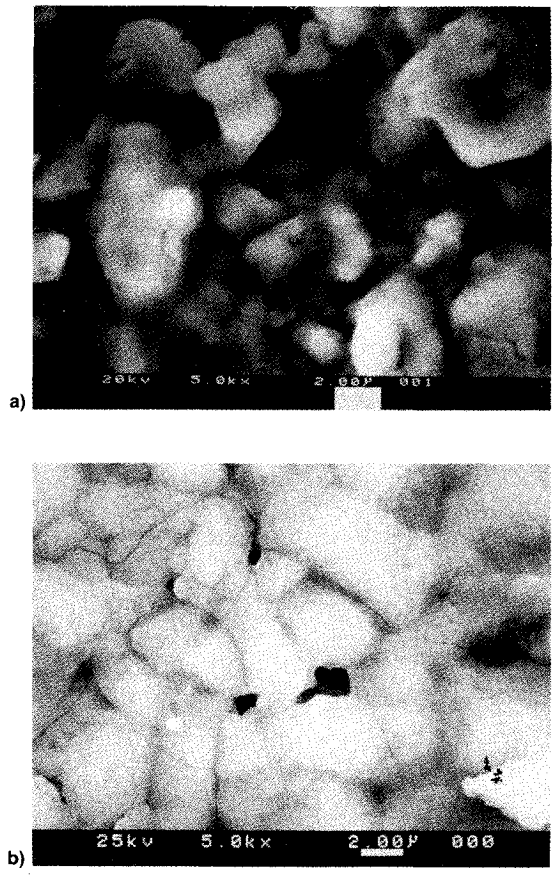


Fig. 9 SEM micrographs of Hexoloy SA a) after 21 h and b) after 73.5 h of oxidation at 1300°C.

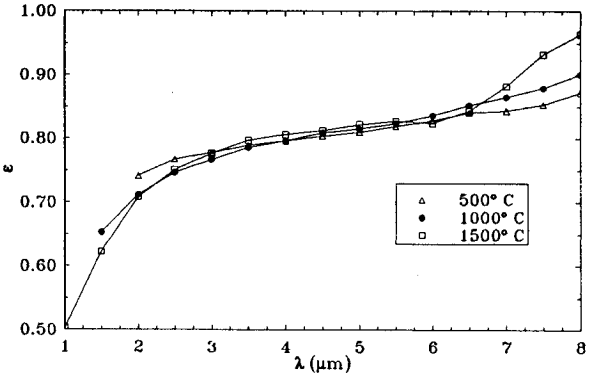


Fig. 10 Normal, spectral emittance of Hexoloy ST (as-received) for various temperatures.

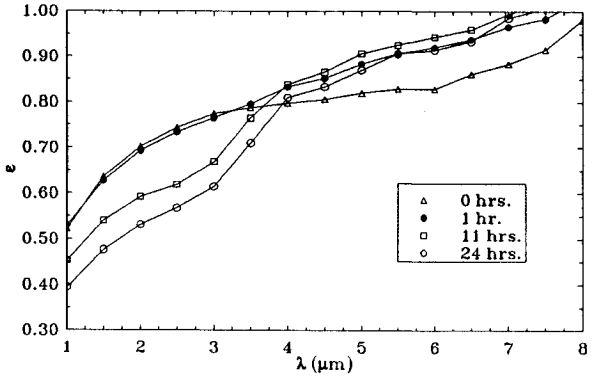


Fig. 11 Normal, spectral emittance of Hexoloy ST for various exposure times to an oxidizing environment at 1300°C.

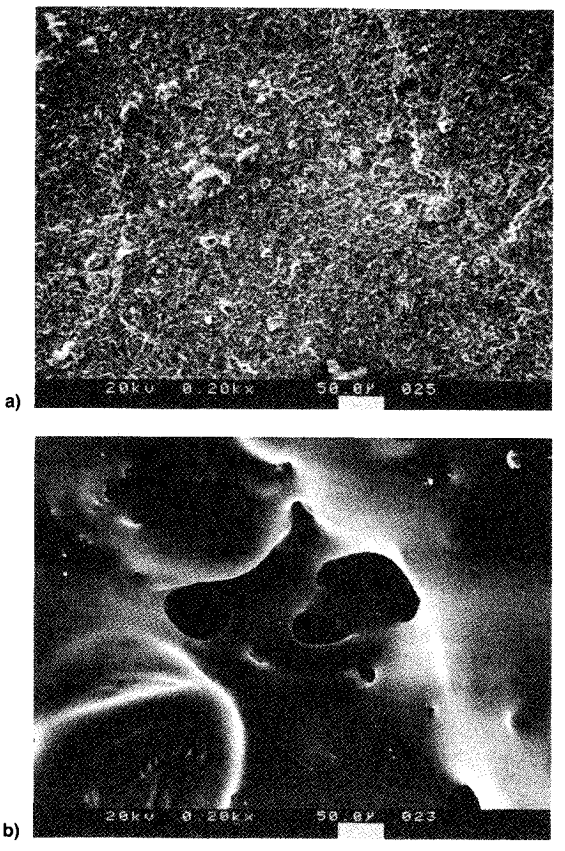


Fig. 12 SEM micrographs of Hexoloy ST a) in the as-received condition and b) following 24 h of oxidation at 1300°C.

silica layer on a silicon carbide substrate can be approximated if both the periodic nature of the material's emittance (as measured from Fig. 8) and the complex index of refraction of the layer and substrate are known.[13] Because the imaginary component of the complex index of refraction is negligible relative to the magnitude of the real component for the silica film and the silicon carbide substrate, the inherent periodic nature in the emittance of the silica layer can be simplified to a function of the film thickness and wavelength

$$\Delta\lambda_0 = \frac{\lambda_0^2}{2n_2 d} \tag{9}$$

In Eq. (9) $\Delta\lambda_0$ is the wavelength interval representing the period of oscillation in the spectral emittance data, $\lambda_0$ represents the spectral location at the midpoint over which $\Delta\lambda_0$ was measured, $n_2$ is the refractive index of the thin layer, and $d$ is the layer thickness. The layer thicknesses approximated through Eq. (9) using the collected emittance data for the oxidized SA samples are in excellent agreement with experimental data collected by Costello and Tressler[17] on the oxidation of silicon carbide. Extrapolated experimental data from Costello and Tressler predict an oxide thickness of 1 $\mu$ after sintered $\alpha$-SiC is exposed to a dry oxygen environment for 75 h. This thickness agrees well with the thickness calculated from Eq. (9) based on the emittance data in Fig. 8.[17] The growth of the oxide layer over time can be observed in Fig. 9. In the micrographs in this figure, the grain boundaries of the SA sample are masked by the growth of a semitransparent silica layer. These boundaries are clearly defined for the unoxidized sample in Fig. 7a and become almost indistinguishable after 73.5 h of oxidation at 1300°C in Fig. 9.

The emittance results collected for Hexoloy ST in the as-received condition displayed virtually no temperature dependence and followed very similar trends relative to the emittance data collected for Hexoloy SA (Fig. 10). The oxidizing results for Hexoloy ST displayed appreciable changes

in emittance as the samples oxidized, as seen from Fig. 11. Inspection of the sample surface indicated extensive oxidation (Fig. 12). The formation of a mixed borosilicate/titania scale on the surface altered the original surface characteristics of the sample. The fine grains evident in Fig. 12a were completely masked over by an amorphous oxide layer, as observed from Fig. 12b. The bubbling of the oxidized surface indicated gas formation at the sample surface.

## Summary

An emissometer was developed to collect emittance data over the spectral range from 1 to 8 $\mu$m for temperatures ranging from 500 to 1500°C. The setup was based on the integral blackbody technique. An FT-IR spectrometer provided a quick and accurate means of signal detection and processing. The sealable sample chamber allowed for the collection of emittance data as a function of exposure time and temperature to a specific environment. The validity of the assumptions associated with the measurement technique were evaluated and verified.

Emittance data were collected for Hexoloy SA and Hexoloy ST samples. The Hexoloy SA samples, which were exposed to carburizing and low-pressure nitrogen ambients displayed only slight variations in emittance when compared to data for samples in the as-received condition. The emittance data for Hexoloy SA samples exposed to oxidizing environments showed slight periodic trends with the growth of an oxide layer. For Hexoloy ST, the emittance data for the as-received samples were very similar to the emittance data for Hexoloy SA. However, a significant change was observed as the surface of the samples oxidized.

## Acknowledgment

Financial support from the Gas Research Institute under Contract 5084-238-1302 is gratefully acknowledged.

## References

[1]Segall, A. E., Hellmann, J. R., and Modest, M. F., "Analysis of Gas-Fired Ceramic Radiant Tubes During Transient Heating: Part I—Thermal Transient Modeling," *Journal of Testing and Evaluation*, Vol. 19, No. 6, 1991, pp. 454–460.

[2]Segall, A. E., and Hellmann, J. R., "Analysis of Gas-Fired Ceramic Radiant Tubes During Transient Heating: Part II—Thermoelastic Stress Analysis," *Journal of Testing and Evaluation*, Vol. 20, No. 1, 1992, pp. 25–32.

[3]Sacadura, J. F., "Measurement Techniques for Thermal Radiation Properties," *Proceedings of the 9th International Heat Transfer Conference*, Hemisphere, Washington, DC, 1990, pp. 207–222.

[4]Touloukian, Y. S., and DeWitt, D. P. (eds.), "Thermal Radiative Properties: Metallic Elements and Alloys," *Thermophysical Properties of Matter*, Vol. 7, Plenum Press, New York, 1970.

[5]Touloukian, Y. S., and DeWitt, D. P. (eds.), "Thermal Radiative Properties: Nonmetallic Solids," *Thermophysical Properties of Matter*, Vol. 8, Plenum Press, New York, 1972.

[6]Touloukian, Y. S., DeWitt, D. P., and Hernicz, R. S. (eds.), "Thermal Radiative Properties: Coatings," *Thermophysical Properties of Matter*, Vol. 9, Plenum Press, New York, 1973.

[7]Chaney, J. F., Ramdas, V., and Rodriquez, C. R. (eds.), *Thermophysical Properties Research Literature Retrieval Guide, 1900–1980*, Plenum Press, New York, 1982.

[8]Richmond, J. C. (ed.), *Measurement of Thermal Radiation Properties of Solids*, NASA SP-31, 1963.

[9]Katzoff, S. (ed.), *Symposium on Thermal Radiation Properties of Solids*, NASA SP-55, 1964.

[10]Knopken, S., and Klemm, R., "Evaluation of Thermal Radiation at High Temperatures," *Measurement of Thermal Radiation Properties of Solids*, edited by J. C. Richmond, NASA SP-31, 1963, pp. 505–514.

[11]Fussell, W. B., and Stair, F., "Preliminary Studies Toward the Determination of Spectral Absorption Coefficients of Homogeneous Dielectric Material in the Infrared at Elevated Temperatures," *Symposium on Thermal Radiation of Solids*, edited by S. Katzoff, NASA SP-55, 1965, pp. 287–292.

[12]Vader, D. T., Viskanta, R., and Incropera, F. P., "Design and Testing of a High-Temperature Emissometer for Porous and Particulate Dielectrics," *Review of Scientific Instruments*, Vol. 57, No. 1, 1986, pp. 87–93.

[13]Modest, M. F., *Radiative Heat Transfer*, McGraw-Hill, New York, 1993.

[14]Gulbransen, E. A., and Jansson, S. A., "The High-Temperature Oxidation, Reduction and Volatilization Reactions of Silicon and Silicon Carbide," *Oxidation of Metals*, Vol. 4, No. 3, 1972, pp. 181–201.

[15]Roy, S., Bang, S. Y., Modest, M. F., and Stubican, V. S., "Measurement of Spectral, Directional Reflectivities of Solids at High Temperatures Between 9 and 11 $\mu$m," *Proceedings of the 3rd ASME/JSME Thermal Engineering Joint Conference*, Vol. 4, 1991, pp. 19–26; also *Applied Optics*, Vol. 32, No. 19, 1993, pp. 3550–3558.

[16]Incropera, F. P., and DeWitt, D. P., *Fundamentals of Heat and Mass Transfer*, 3rd ed., Wiley, New York, 1990.

[17]Costello, J. A., and Tressler, R. E., "Oxidation Kinetics of Silicon Carbide Crystals and Ceramics: I, In Dry Oxygen," *Journal of the American Ceramic Society*, Vol. 69, No. 9, 1986, pp. 674–681.